Dalton Transactions

Cite this: *Dalton Trans.*, 2011, **40**, 6047

www.rsc.org/dalton

PAPER

cis-Dithiolatonickel as metalloligand to dinitrosyl iron units: the di-metallic structure of Ni(μ-SR)[Fe(NO)$_2$] and an unexpected, abbreviated metalloadamantyl cluster, Ni$_2$(μ-SR)$_4$[Fe(NO)$_2$]$_3$†

Chung-Hung Hsieh, Rachel B. Chupik, Scott M. Brothers, Michael B. Hall and Marcetta Y. Darensbourg*

Received 15th March 2011, Accepted 11th April 2011
DOI: 10.1039/c1dt10438a

The reaction of Fe(CO)$_2$(NO)$_2$ and Ni(N$_2$S$_2$) (N$_2$S$_2$ = *N*,*N*′-Bis(2-mercaptoethyl)-1,4-diazacycloheptane) by a single CO replacement yields [Ni(N$_2$S$_2$)]Fe(NO)$_2$(CO), while an excess of Fe(CO)$_2$(NO)$_2$ leads to triply bridging thiolate sulphurs in a cluster of core composition Ni$_2$S$_4$Fe$_3$, lacking one Fe(NO)$_2$ unit to complete the adamantane-like structure. This structural type was earlier identified in a Cu^{I}Cl aggregate of M^{II}(N$_2$S$_2$) (M^{II} = Ni, Cu), in which complete M$^{II}_2$S$_4$Cu$^{I}_4$ core structures were obtained as the major, and, in the case of Cu^{II}(N$_2$S$_2$), the incomplete Cu$^{II}_2$S$_4$Cu$^{I}_3$ as a minor, product. The full Ni$_2$S$_4$Fe$_4$ cluster has not yet been realized for Fe = Fe(NO)$_2$. Computational analysis of the NiFe-heterobimetallic complex addresses structural issues including a ∠Ni–S–Fe of 90° in the bimetallic complex.

Introduction

Inspired by the active sites of enzymes such as acetyl-coA synthase and [NiFe]-hydrogenase, Fig. 1 (a) and (b),[1,2] chemists have explored the *cis*-dithiolatonickel motif as a metalloligand to nickel and to iron, respectively, generating new and interesting S-bridged Ni–Fe structures in the process. In fact, simple synthetic strategies using combinations of Ni^{II}(SR)$_2$ and Ni^{0}L$_2$ or Fe^{II}(CX)$_3$ (X = O, N) synthons have been successful in reproducing the central features of the natural bimetallic sites, Fig. 1 (c), (d) and (e).[3–5] An early [NiFe]-H$_2$ase synthetic analogue utilized the Fe(NO)$_2$ unit as a surrogate for Fe^{II}(CO)(CN)$_2$, generating the Ni–Fe bimetallic structure shown as Fig. 1(f).[6] In the meanwhile, an extensive chemical literature has developed to clarify the intriguing redox and chemical properties of simpler dinitrosyl iron complexes, DNICs, which have significance beyond that of the Fe(NO)$_2$ unit's similarity to Fe^{II}(CO)(CN)$_2$. There is evidence that Fe(NO)$_2$, produced *in vivo* as a result of iron-sulfur cluster degradation by NO, has important physiological properties.[7] The protein-bound (^{protein}Cys-S)$_2$Fe(NO)$_2$ complexes are purported to store NO in high molecular weight forms; when released by free cysteine or glutathione, low molecular weight DNIC's are expected to be NO transport/delivery agents.[8,9] Biomimetic studies of L$_2$Fe(NO)$_2$ complexes have uncovered a rich chemistry that is both NO ligand- and metal-based. The redox properties of DNICs are highly ligand

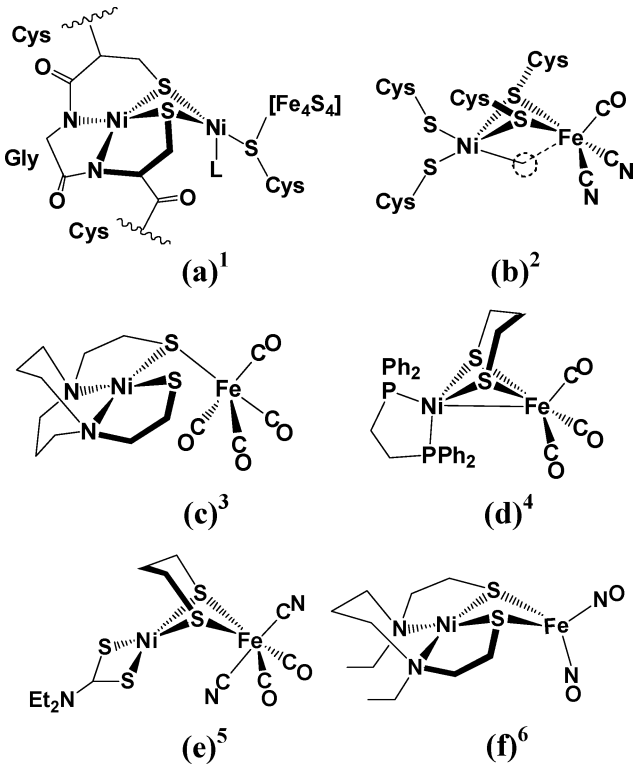

Fig. 1 Structures of the (a) acetyl-coA synthase and (b) [NiFe]-hydrogenase active sites.[1,2] (c-f) Selected model complexes of [NiFe]-hydrogenase active sites.[4–6]

Texas A&M University, 3255 TAMU, College Station, TX, USA. E-mail: marcetta@chem.tamu.edu; Fax: 1 979 845 0158; Tel: 1 979 845 5417

† Electronic supplementary information (ESI) available: X-ray crystallographic data (CIF) from the structure determinations, full listing of metric parameters, X-ray structures, IR studies for complex **1** and **2**, graphical depiction of the vibrational frequencies, and ^{13}C NMR spectrum of complex **1**. CCDC reference numbers 817758 and 817759. For ESI and crystallographic data in CIF or other electronic format see DOI: 10.1039/c1dt10438a

dependent and the NO release structure/function relationships are complicated and remain largely vague.[10–13]

Our interests in codifying the characteristics of $Ni(N_2S_2)$ as metalloligands,[14] and in understanding the ligand-dependent behavior of the $Fe(NO)_2$ and $Fe(NO)_3$ units coincide within the $Ni(N_2S_2)/Fe(NO)_2$ synthetic area.[13,15] Here we report two intriguing discoveries that demonstrate the geometrical preferences and tenacity of the (bismercaptoethane-diazacycloheptane)nickel(II), (bme-dach)Ni, as a metalloligand as it achieves mono- and triply-bridging binding modes to $Fe(NO)_2$.

Results and discussion

The Ni_1Fe_1 complex

The (bme-dach)Ni dithiolate has been shown to bind as a bidentate as well as a monodentate ligand to $W^0(CO)_4$ and $W^0(CO)_5$, respectively.[14,16] Whereas the former adduct, $[\mu_2\text{-}Ni(N_2S_2)]W(CO)_4$, readily adds CO to release one of the bidentate thiolate arms and yield $[\mu\text{-}Ni(N_2S_2)]W(CO)_5$, the pentacarbonyl resists further reaction with CO to completely displace the $Ni(N_2S_2)$ and form $W(CO)_6$. Likewise, the replacement of $Ni(N_2S_2)$ by CO in complex (c), Fig. 1, proceeds only slowly under ambient conditions (days at 1 atm or CO sparge, 22 °C).[3]

Eqn (1) describes the simple CO-displacement reaction that yields a monodentate [(bme-dach)Ni]$Fe(NO)_2(CO)$ complex (**1**); such a product would appear to be the first step towards production of the $Ni(\mu\text{-}SR)_2Fe(NO)_2$ analogue of complex (f), shown in Fig. 1. On mixing the $Fe(CO)_2(NO)_2$ precursor (prepared *in situ* from the reaction of $Fe(CO)_3(NO)^-$ with $NO^+BF_4^-$)[17] with a THF slurry of brown (bme-dach)Ni, a clear brown solution of complex **1** results, which on solvent removal yields a brown crystalline product (*ca.* 60%). The diatomic ligand infrared spectrum of **1** indicates a better donor ligand has replaced CO in the $Fe(CO)_2(NO)_2$ complex; notably in the product the ν(CO) band has shifted to lower wavenumbers (av. 56 cm^{-1}) while the two NO bands show more substantial red shifts (*ca.* 73 cm^{-1}), maintaining their *ca.* 45 cm^{-1} separation.

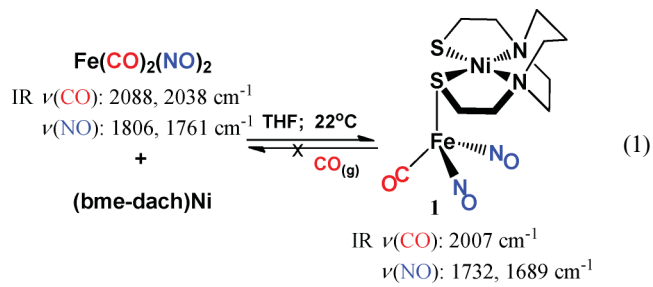

(1)

Single-crystal X-ray diffraction analysis of the black crystalline complex **1**, isolated as described in the experimental section, verified a 4-coordinate, tetrahedral iron, with a single bridging thiolate S, two linear NO's and one CO. Fig. 2 presents two units of the NiFe bimetallic structure as they appear in long range alignment in the packing diagram. Although the average intermolecular distance between nickel and a terminal thiolate sulphur from the nearest neighbour complex is, at 5.3 Å, far beyond van der Waals interactions, the terminal thiolates appear to be positioned so as to potentially interact with the nickel ions in adjacent molecules, Fig. 2. This arrangement has the effect

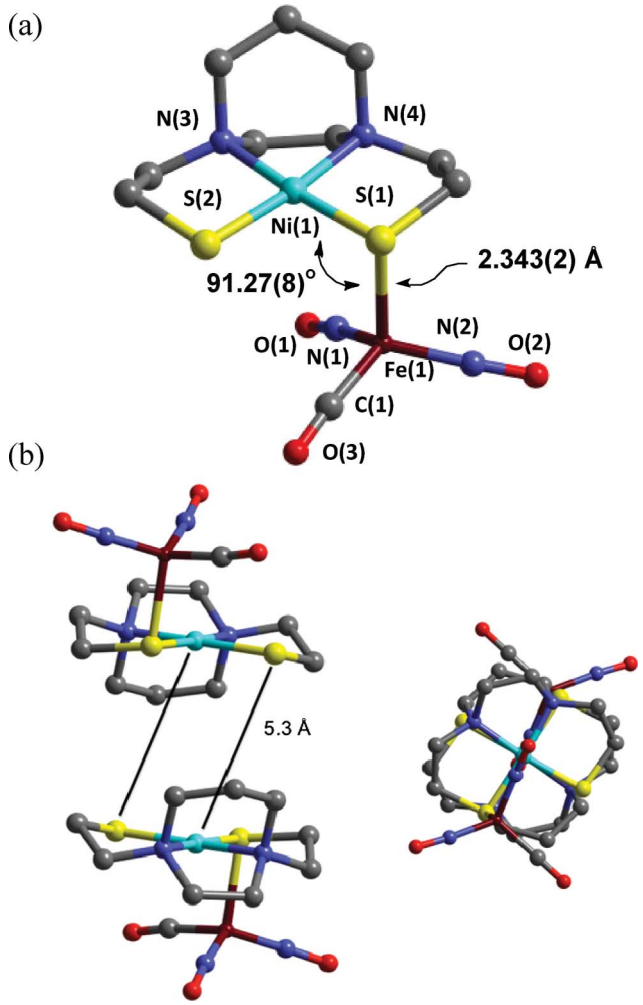

Fig. 2 (a) Ball and stick representation of the molecular structure of [Ni(bme-dach)]$Fe(NO)_2(CO)$ (**1**) (H atoms have been omitted). (b) Views of the pseudo-dimer [Ni(bme-dach)]$Fe(NO)_2(CO)$ as it appears in the packing diagram: side-on, left; down the metal-metal axis, right.

of placing both the diazacycle and the S-bound $Fe(NO)_2(CO)$ groups mutually transoid across the juncture of the two NiN_2S_2 planes, best visualized in the view down the Ni to Ni vector shown in Fig. 2 (b). The tendency of the bme-dach or bme-daco ligands to produce extended structures or coordination polymers *via* S···M···S has been observed in, for example, the (bme-dach)Pt complex solid state structure, where similar alternating alignments continue in a chain.[18] In the case of complex **1**, the pendant $Fe(NO)_2(CO)$ units increase the electrophilicity of the nickel within the heterobimetallic so as to promote the long range interaction with an adjacent unit, but sterically prohibit extended chains (see Fig. S4 in the ESI†).

Selected metric parameters for complex **1** are shown in the structure (Fig. 2) and are listed in Table 1. Of significance is the Ni–Fe distance of 3.229(3) Å of **1**, which is over 0.5 Å shorter than the Ni–Fe distance in structure (c) of Fig. 1. This difference relates to the ∠Ni–S–Fe of the two analogues, 91.3° in **1** and 113.4° in (c). Despite the obvious steric differences arising from (1) the $Ni(N_2S_2)$ metalloligands (the 8-membered diazacyclooctane ring in (c) *vs.* the 7-membered diazacycloheptane ring in complex **1**); and (2) the larger coordination number about the iron in (c) *vs.* **1**,

Table 1 Metric parameters for [(bme-dach)Ni]Fe(NO)$_2$(CO) (complex **1**) (distances Å, angles °)

Fe(1)···Ni(1)	3.229(3)	Ni(1)–S(1)	2.1699(17)
Fe(1)–S(1)	2.3433(19)	Ni(1)–S(2)	2.161(2)
Fe(1)–N(1)	1.701(4)	Ni(1)–N(3)	1.933(3)
Fe(1)–N(2)	1.689(4)	Ni(1)–N(4)	1.940(4)
Fe(1)–C(1)	1.771(5)	C(1)–O(3)	1.151(5)
N(1)–O(1)	1.176(4)	N(2)–O(2)	1.167(5)
Fe(1)–N(1)–O(1)	172.4(3)	S(1)–Ni(1)–S(2)	94.51(6)
Fe(1)–N(2)–O(2)	175.8(4)	N(3)–Ni(1)–N(4)	83.11(14)
Fe(1)–C(1)–O(3)	173.5(3)	S(1)–Ni(1)–N(4)	91.42(11)
S(1)–Fe(1)–N(1)	111.97(12)	S(2)–Ni(1)–N(3)	90.97(11)
S(1)–Fe(1)–N(2)	102.48(14)	N(1)–Fe(1)–N(2)	117.78(17)
S(1)–Fe(1)–C(1)	101.05(12)	Ni(1)–S(1)–Fe(1)	91.27(8)

the magnitude of this ∠Ni–S–Fe difference suggests an electronic effect is also involved. This possibility is explored in on-going computational studies.

Within the Ni(N_2S_2) metalloligand there are no significant metric differences between bound and free forms, as has been noted in other structures in which it serves as a monodentate ligand.[16,19] Likewise, the S-bound pendant iron nitrosyl group has bond distances and angles consonant with other LFe(NO)$_2$(CO) structures, L = NHC (IMes) or PPh_3,[13,20] in which the iron unit is in the diamagnetic, reduced form, {Fe(NO)$_2$}^{10} (Enemark-Feltham notation), as it is in **1**.[21]

As indicated in eqn (1), sparges of CO gas did not return complex **1** to the starting materials under ambient conditions (1 atm, 22 °C). This result is consistent with the strong binding of the nickeldithiolate ligand to $W^0(CO)_5$ and $Fe^0(CO)_4$, demonstrated by a similar non-productive, or very slow, reaction with CO.[3,14,19] Nevertheless, and similar to observations for (c), in the presence of ^{13}C-labeled CO, exchange occurs into complex **1** dissolved in THF solvent. This labeled material was useful for ^{13}C NMR spectra, showing a singlet at 210.07 ppm, illustrative of the diamagnetism of the complex (Fig. S3 in the ESI†).

Computations

The bimetallic complex [Ni(bme-dach)]Fe(NO)$_2$(CO) was probed computationally by a recently developed methodology for complexes containing an iron dinitrosyl unit.[22] A reasonable computational/experimental match of both structural features and diatomic ligand stretching frequencies utilizes the TPSS functional[23a] and a mixed basis set, with the Stuttgart-Dresden parameters and an effective core potential (ECP)[23b] on the iron atom, the LANL2DZ ECP parameters unaugmented on nickel and with an additional d-function on the sulphurs.[23c] For all other atoms, the basis set 6-311++G(d,p) was used. These parameters adequately reproduce the crystallographic metric data, especially in the M–S and M–N bond lengths, which other functional/basis set pairs calculated too long. The salient features of the solid state structure, including the eclipsing of the Fe–N–O bond vector with the Ni–S bond, are computational/experimental matches (see ESI, Fig. S7†); however we note a somewhat larger divergence in the Ni–S–Fe hinge angle, determined to be *ca.* 86° in the calculation *vs.* approximately 91° by experiment. An overlay of the computed and crystallographic structures is shown in Fig. 3.

The experimental, THF solution-phase frequencies for the carbonyl and nitrosyl diatomic ligands were observed at $\nu_{(CO)}$ = 2007 cm^{-1} and ν(NO) = 1732 and 1689 cm^{-1}, whereas the calculated gas-phase frequencies are $\nu_{(CO)}$ = 2001 cm^{-1} and ν(NO) = 1767 (sym.) and 1694 cm^{-1} (asym.). The vibrational frequency at 2001/2007 cm^{-1}, is essentially a carbonyl stretch borrowing minimal intensity from the nitrosyl symmetric stretching vibration leading to an overall dipole oriented along the Fe–C–O vector. In a pseudo-C_{2v} system, which is assumed for other known iron dinitrosyl complexes of the form (L)Fe(NO)$_2$(CO) (where L = CO, N-heterocyclic carbene, *etc.*), the symmetric and asymmetric nitrosyl stretches are expected to draw equal intensity from each nitrosyl. In the bimetallic Ni–Fe(NO)$_2$ complex **1**, one nitrosyl is oriented parallel to a Ni–S bond vector (defined as N–O_{in}) whereas the other is pointed away from the complex (defined as N–O_{out}). As a result of the asymmetry relative to regular C_{2v} complexes, the intensity gained from each nitrosyl in the symmetric and asymmetric stretches varies. The asymmetric stretch at 1694 cm^{-1} displayed a major intensity contribution from Fe–N–O_{in} with a corresponding minor intensity from Fe–N–O_{out}. The symmetric stretch, which was calculated as slightly higher than experiment (1767 *vs.* 1732 cm^{-1}) has its major intensity vector on the Fe–N–O_{out} vibration, drawing a moderate amount of intensity from the carbonyl vibration. A graphical depiction of these frequencies is found in the ESI†.

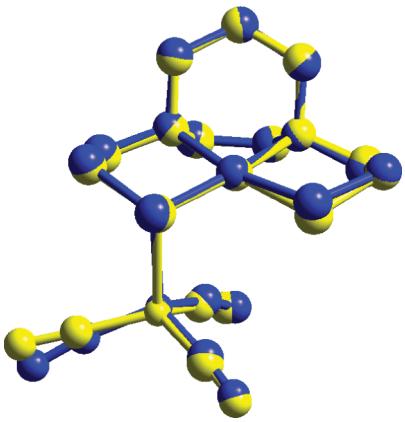

Fig. 3 Overlay of experimental (yellow) and computational (blue) structures of complex **1**.

Among the frontier molecular orbitals (FMOs) of this bimetallic structure, the LUMO, HOMO, and HOMO-1 are mainly comprised of Ni and S character, with little to no contribution from the Fe unit; this manifold has been previously observed in computational studies of typical square planar Ni(N_2S_2) complexes.[24] The three orbitals involved in the *ca.* 90° Ni–S–Fe interaction, which is essentially a Ni_d–S_p–Fe_d orbital manifold with small contributions from the p orbitals of N, C, and O in the Fe(CO)$_2$(NO) moiety, are located below the HOMO-1. The atomic orbitals that make up these three molecular orbitals are as follows: the HOMO-2 is essentially of Fe character, with a smaller percentage of Ni character; the HOMO-3 is the reverse, with mainly Ni character and less Fe character; and the HOMO-4 is nearly equal in Ni and Fe character. A consequence of the energy separation of these delocalized Ni–Fe orbitals and the Ni–S based FMOs is that the HOMO, comprised of largely sulfur character, could be involved in additional S-based reactivity, a prediction corroborated by the formation of the Ni_2Fe_3 cluster described below.

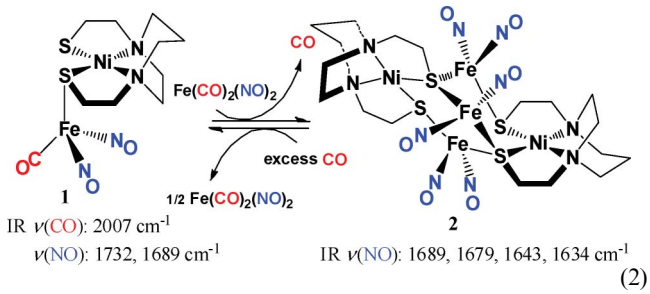

(2)

The Ni_2Fe_3 complex

Under an N_2 purge and in the presence of excess $Fe(CO)_2(NO)_2$, complex **1** converts to $[(bme\text{-}dach)Ni]_2[Fe(NO)_2]_3$, complex **2**, eqn (2). Brown needle-shaped crystals were obtained directly from this reaction mixture on the evaporative removal of solvent and CO under a slow of stream of N_2 overnight. Note that the prominent ν(NO) IR bands of **2** experience major shifts from those of its precursor **1**, eqn (2) and Fig. 5. The diatomic ligand IR data of $LFe(NO)_2(CO)$ where L = PPh_3 and mono-dentate (bme-dach)Ni show that the ν(CO) positions in $LFe(NO)_2(CO)$ are largely the same, 2009 and 2007 cm^{-1}, respectively. However the ν(NO) bands show a greater discrepancy, 1763, 1721 cm^{-1} for L = PPh_3 and 1732, 1689 cm^{-1} for L = (bme-dach)Ni. A similar contrast may be made for $(PPh_3)_2Fe(NO)_2$ and the Ni_2Fe_3 cluster where the ν(NO) band positions are some 30 to 40 cm^{-1} lower in **2** than in $(PPh_3)_2Fe(NO)_2$.[20] Both results are consistent with the better electron-donating ability of the nickel dithiolate *vs.* PPh_3 as established using $W(CO)_{4,5}$ as reporters.[14,20] The point to be made is that the ν(CO) values are much less sensitive to ligand donor ability than are the ν(NO) values in this case. Hence the growing library of ν(NO) values from well characterized $L_2Fe(NO)_2$ in both $\{Fe(NO)_2\}^9$ and $\{Fe(NO)_2\}^{10}$ redox levels should be useful in identifying donor environments within biological milieu.

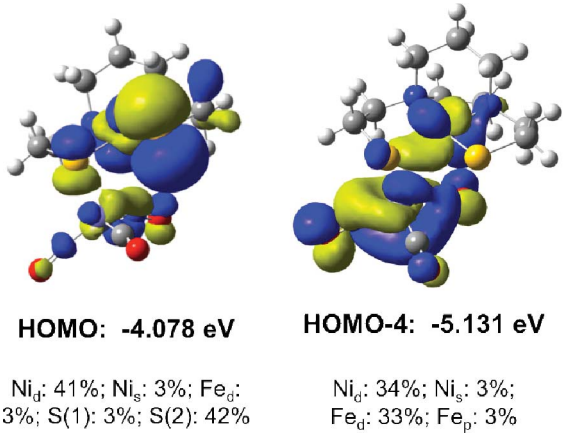

Fig. 4 Selected Frontier Molecular Orbitals (FMOs) of [Ni(bme-dach)]Fe(NO)$_2$(CO), generated at an isosurface value of 0.02. M_d, M_p, and M_s refer to the percentage of *d*, *p*, or *s* orbital character per metal, and S(1) refers to the bridging Ni–S–Fe sulfur, whereas S(2) is the terminal Ni–S thiolate.

Fig. 6 displays the ball and stick representation of the molecular structure from the single-crystal X-ray diffraction analysis of complex **2** and the selected bond distances and angles are listed in Table 2. The structure consists of two six-membered NiS_3Fe_2 cyclohexane-like rings in chair conformations and one eight-membered $Ni_2S_4Fe_2$ ring held within an incomplete adamantane-like cluster. The six Fe–S distances within the cluster are statistically the same, averaging to 2.313 Å. Likewise the small difference in Ni–S distances are well within 3σ and average to 2.169 Å. The metric data within the $Ni(N_2S_2)$ unit acting as a ligand to $Fe(NO)_2$ are the same as those found in the free (bme-dach)Ni. In both, the ∠S–Ni–S is *ca.* 96° and the ∠N–Ni–N is *ca.* 83°. This consistency of data verifies the rigidity of the (bme-dach)Ni as a building block in cluster formation.[25]

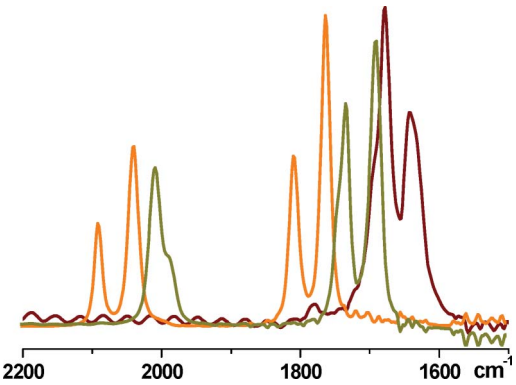

Fig. 5 Overlaid IR spectra of $Fe(CO)_2(NO)_2$ [orange: ν(CO) 2088 (m), 2038 (s); ν(NO) 1806 (m), 1761 (s)], complex **1** [olive green: ν(CO) 2007 (m), ν(NO) 1732 (m), 1689 (s)] and complex **2** [wine red: ν(NO) 1689 (sh), 1679 (vs), 1643 (s), 1634 (sh)].

An analogous structure was earlier identified in a $[Cu^{II}(N_2S_2)]_2[Cu^{I}Cl]_3$ heterometallic aggregate, Fig. 7 (b), formed by the simple combination of $Cu^{I}Cl$ with $Cu^{II}(N_2S_2)$. The major product of this reaction, as well as that from a similar reaction with nickel (with nearly identical structures), was the completed adamantane-like cluster, $[M^{II}(N_2S_2)]_2[CuCl]_4$, Fig. 7 (a).[26] In these complexes the $M(N_2S_2)$ unit was based on (bme*-daco)M, bme*-daco = bis(*N*,*N*′-2-mercapto-2-methylpropyl)-1,

Table 2 Metric parameters for $[(bme\text{-}dach)Ni]_2[Fe(NO)_2]_3$ (complex **2**) (distances Å, angle °)

Fe(1)–N(1)	1.650(12)	Ni(1)–S(1)	2.179(3)
Fe(1)–N(2)	1.623(10)	Ni(1)–S(2)	2.171(3)
Fe(2)–N(3)	1.651(11)	Ni(2)–S(3)	2.162(3)
Fe(2)–N(4)	1.614(11)	Ni(2)–S(4)	2.163(3)
Fe(3)–N(5)	1.614(11)	Ni(1)–N(7)	1.968(10)
Fe(3)–N(6)	1.656(11)	Ni(1)–N(8)	1.912(9)
Fe(1)–S(1)	2.320(3)	Fe(1)–S(4)	2.323(4)
Fe(2)–S(1)	2.323(3)	Fe(2)–S(3)	2.305(4)
Fe(3)–S(2)	2.309(3)	Fe(3)–S(3)	2.298(3)
Ni(2)–N(9)	1.942(10)	Ni(2)–N(10)	1.939(9)
N(1)–O(1)	1.184(13)	N(2)–O(2)	1.226(13)
N(3)–O(3)	1.183(13)	N(4)–O(4)	1.219(12)
N(5)–O(5)	1.215(12)	N(6)–O(6)	1.205(11)
Fe(1)–N(1)–O(1)	167.9(10)	Fe(1)–N(2)–O(2)	170.5(10)
Fe(2)–N(3)–O(3)	170.4(10)	Fe(2)–N(4)–O(4)	171.8(10)
Fe(3)–N(5)–O(5)	177.3(9)	Fe(3)–N(6)–O(6)	172.2(9)
S(1)–Ni(1)–S(2)	97.68(12)	N(7)–Ni(1)–N(8)	83.0(4)
S(3)–Ni(2)–S(4)	94.84(13)	N(9)–Ni(2)–N(10)	82.5(4)
S(1)–Fe(1)–S(4)	94.02(12)	S(1)–Fe(2)–S(3)	91.47(12)
S(2)–Fe(3)–S(3)	96.69(12)	N(1)–Fe(1)–N(2)	115.8(5)
N(3)–Fe(2)–N(4)	120.7(5)	N(5)–Fe(3)–N(6)	121.6(5)

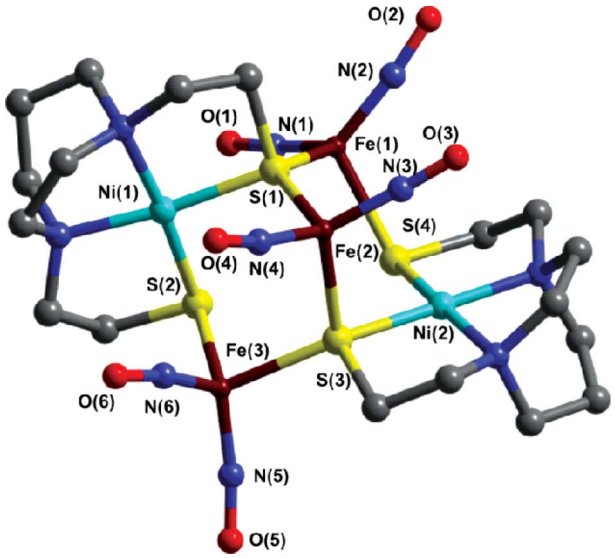

Fig. 6 Ball and stick representation of the molecular structure of $[(bme\text{-}dach)Ni]_2[Fe(NO)_2]_3$ (**2**) (THF solvent molecule of crystallization and H atoms have been omitted).

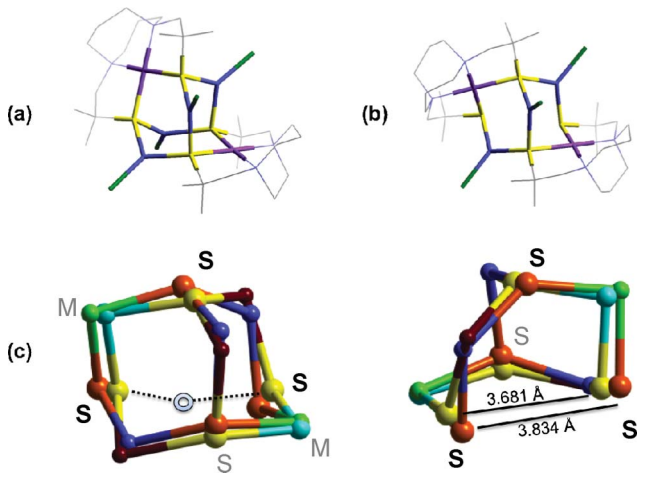

Fig. 7 (a) $[M^{II}(N_2S_2)]_2[Cu^{I}Cl]_4$ (M = Ni, Cu) with the adamantane core highlighted. (b) $[M^{II}(N_2S_2)]_2[Cu^{I}Cl]_3$ (M = Cu) with the adamantane core highlighted. (c) Adamantane core overlays of $[Cu^{II}(N_2S_2)]_2[Cu^{I}Cl]_3$ (blue Cu^{I}, orange: S, green: Cu^{II}) and $[Ni(N_2S_2)]_2[Fe(NO)_2]_3$ (red: Fe, yellow: S, light blue: Ni). = vacant site in the adamantane core.

5-diazocyclooctane, with steric hindrance positioned on the carbon α to sulfur. In that complex and in complex **2**, the MS_2 units form the opposite apices of the adamantane-like cluster, with the MS_2 planes roughly perpendicular to each other. The overlay of the adamantane-like cores of **2** and the analogous $[Cu^{II}(N_2S_2)]_2[Cu^{I}Cl]_3$ is also shown in Fig. 7 (c). The vacant site is illustrated by the open circle; in a rotated view the possibility of binding a 4th metal is suggested, a possibility that was realized for $Cu^{I}Cl$ but not for $Fe(NO)_2$. Attempts to achieve the latter have thus far been unsuccessful. Preliminary computations on a small model of this cluster suggest that the vacant site cannot accommodate an additional $Fe(NO)_2$ unit.

Reactivity of complex 2 with $CO_{(g)}$

A reactivity property of the Ni_2Fe_3 complex is that under 1 atm (excess) CO, the cluster is converted to complex **1** along with 0.5 equiv. of $Fe(CO)_2(NO)_2$, eqn (2). Note that CO displacement of the $Ni(N_2S_2)$ metalloligand from the pure isolated complex **1** did not occur at 22 °C, eqn (1). We posit that within complex **2** one of the $Fe(NO)_2$ units, that designated as Fe(2) in Fig. 6, is more labile than the others. The reason for this could lie in the fact that both of the sulfurs binding to Fe(2) are triply bridging, whereas for Fe(1) and Fe(3), one sulfur is μ_3 and one is a typical μ_2 bridge bond. Hence the Fe–μ_3-SR–Ni bonds could be broken and replaced by CO, while the Fe–μ_2-SR–Ni bond is maintained, binding tenaciously to $Fe(NO)_2(CO)$ as seen in the $[Ni(N_2S_2)]W(CO)_5$ and $[Ni(N_2S_2)]Fe(CO)_4$ cases described above.[3,19]

Experimental

General information

All reactions and operations were carried out on a double-manifold Schlenk vacuum line or in a glove box under either a N_2 or an Ar atmosphere. THF, CH_2Cl_2, pentane and diethyl ether were freshly purified by an MBraun Manual Solvent Purification System packed with Alcoa F200 activated alumina desiccant. The purified THF, CH_2Cl_2, pentane and diethyl ether were stored with molecular sieves under N_2 before experiments. The known complexes $Fe(CO)_2(NO)_2$ and [(bme-dach)Ni], bme-dach = *N*,*N*′-bis(2-mercaptoethyl)-1,4-diazacycloheptane) were synthesized by published procedures.[17,25] The following materials were of reagent grade and were used as purchased from Sigma-Aldrich or TCI: $Fe(CO)_5$, nitrosyl tetrafluoroborate, 18-crown 6-ether (CE).

Physical measurements

^{13}C NMR spectra were measured on a Unity+ 300 MHz superconducting NMR instrument. Solution infrared spectra were recorded on a Bruker Tensor 27 FTIR spectrometer using 0.1 mm KBr sealed cells. Elemental analyses were performed by Atlantic Microlab, inc., Norcross, Georgia, USA.

X-Ray crystal structure analyses

A Bausch and Lomb 10 x microscope was used to identify suitable crystals of the same habit. Each crystal was coated in paratone, affixed to a Nylon loop and placed under streaming nitrogen (110 K) in a SMART Apex CCD diffractometer or Bruker Gadds (see details in .cif files†). The space groups were determined on the basis of systematic absences and intensity statistics. The structures were solved by direct methods and refined by full-matrix least squares on F^2. Anisotropic displacement parameters were determined for all nonhydrogen atoms. Hydrogen atoms were placed at idealized positions and refined with fixed isotropic displacement parameters. The following is a list of programs used: data collection and cell refinement, SMART WNT/2000 Version 5.632, APEX 2 or FRAMBO Version 4.1.05 (GADDS);[27,31] data reductions, SAINTPLUS Version 6.63;[28] absorption correction, SADABS;[29] structural solutions, SHELXS-97;[30] structural refinement, SHELXL-97;[31] graphics and publication materials, Mercury.[32]

Computations

Computations were performed using the Gaussian 09 software suite,[33] with the crystallographic parameters used as the starting input structure under a variety of different functional/basis set pairs. The TPSS functional[23] as well as a mixed basis set described above were utilized for final optimizations, and a separate frequency calculation was performed to ascertain a stable structure with the absence of imaginary frequencies. The Ampac Graphical User Interface (AGUI)[34] was used to general molecular orbitals, and Cerius2 was used to render the overlay structure.[35]

Synthesis of [(bme-dach)Ni]Fe(NO)$_2$(CO) (1)

$Fe(CO)_2(NO)_2$ was freshly prepared by the addition of [Na-CE][$Fe(CO)_3(NO)$] (0.55 g, 1.2 mmol) and [NO]BF_4 (0.14 g, 1.2 mmol) to THF (20 mL) at room temperature. The mixture was stirred for 10 min, and the product within the solution was vacuum transferred into a Schlenk flask maintained at liquid N_2 temperature. The resulting purified product/solution was a clear orange color. A sample of Ni(bme-dach) (0.22 g, 0.8 mmol) was weighed into a second Schlenk flask, THF was added (20 mL), and the resulting dark yellow/brown solution was stirred for 10 min prior to the addition of the purified $Fe(CO)_2(NO)_2$ solution *via* cannula. After stirring for 2 h, an IR spectrum taken of this solution indicated the formation of complex **1**. IR ν(CO): 2007 (m); ν(NO): 1732 (m), 1689 (s) (THF, cm^{-1}) and none of the starting material, $Fe(CO)_2(NO)_2$, remained. The solution was then filtered through celite to remove solids and pentane was added to the filtrate to yield a brown precipitate, which was washed with portions of pentane (3 × 10 mL), yield: 0.21 g, 63%. Black, needle shaped crystals suitable for single crystal X-ray diffraction were obtained on pentane diffusion into a THF solution at –35 °C. IR ν(CO): 2007 (m); ν(NO): 1732 (m), 1689 (s) (THF, cm^{-1}). Elem. anal., found (calcd for $C_{10}H_{18}FeN_4NiO_3S_2$)%: C 28.67 (28.53), H 4.66 (4.31), N 13.29 (13.31).

Exposure of complex 1 to CO$_{(g)}$

Complex **1** (0.04 g, 0.1 mmol) was loaded into a Schlenk flask and dissolved in THF (20 mL). Carbon monoxide was then bubbled in for 10 min. An IR spectrum was immediately taken but revealed no change in the spectrum from that of complex **1**. Under a blanket of CO, the solution was stirred overnight, with no change observed in the IR spectrum. Isotopic enrichment was obtained by bubbling ^{13}CO into a Schlenk flask containing 1 equiv. of complex **1** dissolved in THF (20 mL) for 1 min. The IR spectrum showed a new band at ν(CO) 1962 (calcd 1961 from reduced mass) cm^{-1} while there was no change in the NO peaks.

Synthesis of [Ni(bme-dach)]$_2$[Fe(NO)$_2$]$_3$ (2)

To a Schlenk flask containing complex **1** (0.17 g, 0.4 mmol) in THF (20 mL) was added freshly prepared $Fe(CO)_2(NO)_2$ (0.03 g, 0.2 mmol) in THF. The reaction mixture was stirred for 10 min and then purged with nitrogen overnight. The resulting dark red, brown solid with some needle shaped crystals was insoluble in THF, which was added (3 × 10 mL) to remove impurities from the product, **2**. An IR spectrum revealed no starting material remained, yield: 0.05 g, 28%. IR ν(NO): 1689 (sh), 1679 (s), 1643 (m), 1634 (sh) (CH_2Cl_2, cm^{-1}). Elem. anal., found (calc'd for $C_{18}H_{36}Fe_3N_{10}Ni_2O_6S_4$)%: C 23.94 (23.98), H 4.52 (4.02), N 15.24 (15.53).

Reaction of complex 2 with CO$_{(g)}$

Complex **2** (0.09 g, 0.1 mmol) was loaded into a Schlenk flask and dissolved in CH_2Cl_2 (20 mL). Carbon monoxide was then bubbled in for 10 min. The solution was sealed under a CO atmosphere and stirred overnight at 22°. The IR spectral monitor revealed a change from the two absorbances of complex **2** to multiple bands indicating a mixture of complex **1** and $Fe(CO)_2(NO)_2$.

Conclusions

By virtue of the Ni(d_π)-S(p_{π^*}) interaction, Ni–SR bonds are activated towards reaction with electrophiles, typically with maintenance of the Ni–S bonds and the integrity of the coordination sphere. Well known macrocycle templated reactions have been based on the reaction of *cis*-dithiolate complexes of nickel with the α-Ω organic halides. In the Ni_2Fe_3 complex described here, the dithiolate is shown to template cluster formation with metallo-electrophiles. In the case of $\{Fe(NO)_2\}^{10}$, two sites require donor ligands to complete its 4-coordinate tetrahedral geometry preference. Thus, using independent and rigid $M^{II}(N_2S_2)$ units as donors, and the ability of the thiolate ligand to triply bridge metals, a cluster formation approaching the classical adamantane geometry is realized. The interesting convergence of structural forms from both Cu^ICl and $\{Fe(NO)_2\}^{10}$ reflects their similar electrophilicities, especially towards thiolato sulfurs. That the trigonal geometrical preferences of Cu^I and the tetrahedral preferences of the $Fe(NO)_2$ could yield the same overall cluster geometry was not, however, predicted, *a priori*. The availability of the vacant site in the cluster for exogenous metal binding suggests additional efforts in the synthesis of heterometallic clusters.

Acknowledgements

We appreciate financial support from the National Science Foundation (CHE-0910679 to MYD and CHE-0910552 to MBH) and the R. A. Welch Foundation (A-0924 to MYD and A-0648 to MBH). We also thank Dr Joseph H. Reibenspies (TAMU) for assistance with X-ray studies.

Notes and references

1 C. Darnault, A. Volbeda, E. J. Kim, P. Legrand, X. Vernède, P. A. Lindahl and J. C. Fontecilla-Camps, *Nat. Struct. Biol.*, 2003, **10**, 271.
2 J. C. Fontecilla-Camps, A. Volbeda, C. Cavazza and Y. Nicolet, *Chem. Rev.*, 2007, **107**, 4273.
3 C.-H. Lai, J. H. Reibenspies and M. Y. Darensbourg, *Angew. Chem., Int. Ed. Engl.*, 1996, **35**, 2390.
4 W. Zhu, A. C. Marr, Q. Wang, F. Neese, D. J. E. Spencer, A. J. Blake, P. A. Cooke, C. Wilson and M. Schröder, *Proc. Natl. Acad. Sci. U. S. A.*, 2005, **102**, 18280.
5 Z. L. Li, Y. Ohki and K. Tatsumi, *J. Am. Chem. Soc.*, 2005, **127**, 8950; Y. Ohki, K. Yasumura, M. Ando, S. Shimokata and K. Tatsumi, *Proc. Natl. Acad. Sci. U. S. A.*, 2010, **107**, 3994.
6 F. Osterloh, W. Saak, D. Haase and S. Pohl, *Chem. Commun.*, 1997, 979.
7 A. F. Vanin, V. D. Mikoyan and L. H. Kubrina, *Biophysics*, 2010, **55**, 5.
8 M. W. Foster and J. A. Cowan, *J. Am. Chem. Soc.*, 1999, **121**, 4093.

9 (*a*) H. Ding and B. Demple, *Proc. Natl. Acad. Sci. U. S. A.*, 2000, **97**, 5146; (*b*) W. Yang, P. A. Rogers and H. Ding, *J. Biol. Chem.*, 2002, **277**, 12868.

10 M.-C. Tsai, F.-T. Tsai, T.-T. Lu, M.-L. Tsai, Y.-C. Wei, I.-J. Hsu, J.-F. Lee and W.-F. Liaw, *Inorg. Chem.*, 2009, **48**, 9579.

11 R. Wang, X. Wang, E. B. Sundberg, P. Nguyen, G. P. G. Grant, C. Sheth, Q. Zhao, S. Herron, K. A. Kantardjieff and L. Li, *Inorg. Chem.*, 2009, **48**, 9779.

12 C. E. Tinberg, Z. J. Tonzetich, H. Wang, L. H. Do, Y. Yoda, S. P. Cramer and S. J. Lippard, *J. Am. Chem. Soc.*, 2010, **132**, 18168.

13 C.-H. Hsieh and M. Y. Darensbourg, *J. Am. Chem. Soc.*, 2010, **132**, 14118; C.-Y. Chiang, M. L. Miller, J. H. Reibenspies and M. Y. Darensbourg, *J. Am. Chem. Soc.*, 2004, **126**, 10867; C.-Y. Chiang and M. Y. Darensbourg, *JBIC, J. Biol. Inorg. Chem.*, 2006, **11**, 329.

14 M. V. Rampersad, S. P. Jeffery, M. L. Golden, J. Lee, J. H. Reibenspies, D. J. Darensbourg and M. Y. Darensbourg, *J. Am. Chem. Soc.*, 2005, **127**, 17323.

15 W.-F. Liaw, C.-Y. Chiang, G.-H. Lee, S.-M. Peng, C.-H. Lai and M. Y. Darensbourg, *Inorg. Chem.*, 2000, **39**, 480.

16 S. P. Jeffery, M. L. Singleton, J. H. Reibenspies and M. Y. Darensbourg, *Inorg. Chem.*, 2007, **46**, 179.

17 D. W. McBride, S. L. Stafford and F. G. A. Stone, *Inorg. Chem.*, 1962, **1**, 386.

18 E. Almaraz, Q. A. de Paula, Q. Liu, J. H. Reibenspies, M. Y. Darensbourg and N. P. Farrell, *J. Am. Chem. Soc.*, 2008, **130**, 6272.

19 A. L. Phelps, M. V. Rampersad, S. B. Fitch, M. Y. Darensbourg and D. J. Darensbourg, *Inorg. Chem.*, 2006, **45**, 119.

20 F. I. Atkinson, H. E. Blackwell, N. C. Brown, N. G. Connelly, J. G. Crossley, A. G. Orpen, A. L. Rieger and P. H. Rieger, *J. Chem. Soc., Dalton Trans.*, 1996, 3491.

21 J. H. Enemark and R. D. Feltham, *Coord. Chem. Rev.*, 1974, **13**, 339.

22 S. M. Brothers, M. Y. Darensbourg and M. B. Hall, *Manuscript in Preparation.*.

23 (*a*) J. M. Tao, J. P. Perdew, V. N. Staroverov and G. E. Scuseria, *Phys. Rev. Lett.*, 2003, **91**, 146401; (*b*) J.-D. Chai and M. Head-Gordon, *Phys. Chem. Chem. Phys.*, 2008, **10**, 6615; (*c*) C. E. Check, T. O. Faust, J. M. Bailey, B. J. Wright, T. M. Gilbert and L. S. Sunderlin, *J. Phys. Chem. A*, 2001, **105**, 8111.

24 A. Dey, K. N. Green, R. M. Jenkins, S. P. Jeffrey, M. Y. Darensbourg, K. O. Hodgson, B. Hedman and E. I. Solomon, *Inorg. Chem.*, 2007, **46**, 9655; K. N. Green, S. M. Brothers, R. M. Jenkins, C. E. Carson, C. A. Grapperhaus and M. Y. Darensbourg, *Inorg. Chem.*, 2007, **46**, 7536; C. S. Mullins, C. A. Grapperhaus and P. M. Kozlowski, *JBIC, J. Biol. Inorg. Chem.*, 2006, **11**, 617.

25 J. J. Smee, M. L. Miller, C. A. Grapperhaus, J. H. Reibenspies and M. Y. Darensbourg, *Inorg. Chem.*, 2001, **40**, 3601.

26 M. L. Miller, S. A. Ibrahim, M. L. Golden and M. Y. Darensbourg, *Inorg. Chem.*, 2003, **42**, 2999.

27 *APEX2 V2009.7-0*, Bruker AXS Inc., 5465 East Cheryl Parkway, Madison, WI, 53711–5373, USA, 2007.

28 *SAINT V6.63, Program for Reduction of Area Detector Data*, Bruker AXS Inc., 5465 East Cheryl Parkway, Madison, WI, 53711–5373, USA.

29 G. M. Sheldrick, *SADABS, Program for area detector adsorption correction*, Institute for Inorganic Chemistry, University of Göttingen, Germany, 1996.

30 G. M. Sheldrick, *SHELXS-97, Program for solution of crystal structures*, University of Göttingen, Germany, 1997.

31 *FRAMBO:FRAME Buffer Operation Version 41.05, Program for Data Collection on Area Detectors*, Bruker AXS Inc., Madison, WI, 1999.

32 F. Macrae, P. R. Edgington, P. McCabe, E. Pidcock, G. P. Shields, R. Taylor, M. Towler and J. van de Streek, "Mercury: visualization and analysis of crystal structures", *J. Appl. Crystallogr.*, 2006, **39**, 453.

33 M. J. Frisch, G. W. Trucks, H. B. Schlegel, G. E. Scuseria, M. A. Robb, J. R. Cheeseman, G. Scalmani, V. Barone, B. Mennucci, G. A. Petersson, H. Nakatsuji, M. Caricato, X. Li, H. P. Hratchian, A. F. Izmaylov, J. Bloino, G. Zheng, J. L. Sonnenberg, M. Hada, M. Ehara, K. Toyota, R. Fukuda, J. Hasegawa, M. Ishida, T. Nakajima, Y. Honda, O. Kitao, H. Nakai, T. Vreven, J. A. Montgomery, Jr., J. E. Peralta, F. Ogliaro, M. Bearpark, J. J. Heyd, E. Brothers, K. N. Kudin, V. N. Staroverov, R. Kobayashi, J. Normand, K. Raghavachari, A. Rendell, J. C. Burant, S. S. Iyengar, J. Tomasi, M. Cossi, N. Rega, J. M. Millam, M. Klene, J. E. Knox, J. B. Cross, V. Bakken, C. Adamo, J. Jaramillo, R. Gomperts, R. E. Stratmann, O. Yazyev, A. J. Austin, R. Cammi, C. Pomelli, J. Ochterski, R. L. Martin, K. Morokuma, V. G. Zakrzewski, G. A. Voth, P. Salvador, J. J. Dannenberg, S. Dapprich, A. D. Daniels, O. Farkas, J. B. Foresman, J. V. Ortiz, J. Cioslowski and D. J. Fox, *GAUSSIAN 09 (Revision A.1)*, Gaussian, Inc., Wallingford, CT, 2009.

34 AMPAC(tm) 9, Semichem, Inc., 12456 W 62nd Terrace - Suite D, Shawnee, KS 66216, 1992–2008.

35 *Cerius2*, version 3.0, MSI, Cambridge, U.K.